Deep Learning-Based Classification of Plant Xylem Tissue from Light Micrographs

Sean Wu[1(✉)], Reem Al Dabagh[1], Anna L. Jacobsen[2], Helen I. Holmlund[1], and Fabien Scalzo[1,3]

[1] Seaver College, Pepperdine University, Malibu, CA 90265, USA
sean.wu@pepperdine.edu
[2] California State University Bakersfield, Bakersfield, CA 93311, USA
[3] Department of Computer Science, University of California, Los Angeles (UCLA), Los Angeles, CA 90095, USA

Abstract. Anatomical studies of plant hydraulic traits have traditionally been conducted by manual measurements of light micrographs. An automated process could expedite analysis and broaden the scope of questions that can be asked, but such an approach would require the ability to accurately classify plant cells according to their type. Our research evaluates a deep learning-based model which accepts a cropped cell image input alongside a broader cropped image which incorporates contextual information of that cell type's original cropped image, and learns to segregate these plant cells based off of the features of both inputs. Whilst a single cropped image classification yielded adequate results with outputs matching the ground-truth labels, we discovered that a second image input significantly bolstered the model's learning and accuracy (98.1%), indicating that local context provides important information needed to accurately classify cells. Finally our results imply a future application of our classifier to automatic cell-type detection in xylem tissue image cross sections.

1 Introduction

Plants are important global producers of oxygen and they serve as an important food source for many animals. This makes plants essential for the existence of most life on Earth. Most plant life on land is limited to some extent by water availability. While most plants have some basic adaptations to control water loss (such as a waxy cuticle covering the leaves and the ability to regulate water loss through stomata), some plants have adapted to thrive in dry regions such as the desert and chaparral ecosystems of southern California [1,2]. During drought, some of the most dehydration tolerant chaparral shrubs can survive internal water pressures that are more negative than −10 MPa, absolute pressures that are equivalent to approximately 100 times Earth's atmospheric pressure [3,4].

The ability of some plants to survive extreme dehydration is attributed in part to anatomical characteristics of the plant vascular tissue system. The

G. Bebis et al. (Eds.): ISVC 2022, LNCS 13598, pp. 237–248, 2022.
https://doi.org/10.1007/978-3-031-20713-6_18

vascular tissue system is composed, in part, of xylem. Xylem tissue transports water from the roots to the leaves. The xylem tissue contains several cell types with distinct functions [5], that may be divided into three cellular classifications. 1) Tracheary elements are elongate tubes with a large diameter for the passive transport of water, which is pulled through the plant by evaporation from the leaves (i.e., transpiration). They have a thick secondary cell wall and are dead upon maturity, facilitating their function of long-distance transport. There are two types of tracheary elements that may be found within chaparral shrubs, vessel elements and tracheids. 2) Fibers are also elongate cells, but they function primarily as mechanical support for the stem or root by means of their thick cell walls with a narrow lumen. 3) Parenchyma cells are short cells that have thin primary cell walls and are typically alive at maturity. They function in short-distance transport and storage of water and starch (long-term sugar reserves). There are two types of parenchyma cells that may occur within the xylem, axial parenchyma and ray parenchyma. While all flowering plants have these three cell types present in the xylem, structural adaptations within each cell type can improve whole-plant dehydration tolerance. Additionally, different species may differ greatly in the proportions of these cell type classes within their xylem, with the amount of different cell type classes linked to differences in plant function [6,7].

Small changes in xylem cell characteristics can have a large impact on their function. For example, there is a tradeoff between hydraulic efficiency (which contributes to greater sugar production and growth) and resistance to freezing-induced gas bubble (embolism) formation in the vascular system (which can lead to whole-plant mortality), with large diameter tracheary elements being efficient but highly vulnerable to embolism [8–10]. In a similar way, tracheary element implosion resistance (measured as the cell wall thickness to breadth ratio, $(t/b)^2$) also corresponds to dehydration-induced embolism resistance [11,12]. Although not directly conducting water, the fibers provide mechanical support (estimated by parameters such as wall thickness and lumen diameter) that increases embolism resistance and the mechanical strength of the stem [2,12]. The proportion of the parenchyma within the xylem can indicate the plant's relative carbon stores, with implications for tradeoffs related to carbon starvation and drought tolerance [5,6,13].

Traditionally, all these measurements related to plant anatomy have been taken manually or semi-automatically from light micrographs of transverse stem sections. However, given the difficulty of scaling up time-intensive measurements to whole ecosystems or the globe, it is compelling to find faster ways to measure key xylem traits without compromising accuracy. There is a need for automated, scalable software tools that could automatically analyze large datasets efficiently. An accurate but automated way to measure anatomical traits could also allow us to take advantage of increasingly available large image datasets [14]. In short, a faster means of measuring key characteristics of xylem anatomy would greatly broaden the scope of questions that can be asked about plant structure and function. We tackle this problem in this paper by introducing a deep learning-based model for classification of plant cells.

2 Related Works

In recent years, cell type classification with machine learning has received significant attention particularly in the medical field. Researchers have made breakthrough findings in cancer cell type classifications [15] and cardiovascular research [16], for example, where different types of white blood cells were segregated through popular machine learning techniques such as Deep Learning, or a Random Forest algorithms [17].

Although some prior studies have used semi-automated approaches to classify plant cells [18], and there exists commercially available software such as WinCELL (Regent Instruments, Inc.), there are relatively few previous applications of machine learning to plant hydraulic anatomy. Previous studies have applied machine learning algorithms to topics such as plant disease classification [19] and plant leaf classification [20]; however few studies have been conducted on machine learning at the cellular level. Those studies at this microscopic level have mainly been focused on the segmentation of plant tissues, then possibly classifying those segmented images [14,21–24]. To our best knowledge, we are the first group to design a cascade-like machine learning model to classify tracheary elements (vessels), fibers, and parenchyma cells in plants, with discussions on the effects of inputting a contextualized image alongside the image to be classified.

3 Dataset and Problem Definition

Our dataset for this project consists of light micrographs of transverse stem and root sections of three chaparral shrub species native to the Santa Monica Mountains in southern California: *Ceanothus crassifolius* (CCR), *Ceanothus oliganthus* (CO), and *Frangula californica* (FCA). The samples were collected in 2007 at Cold Creek Canyon (34°05′36.0″N, 118°39′02.9″W). Samples were taken from three individuals of each species to account for genetic and phenotypic variation among individuals. Thin circular slices of the stems and roots (transverse sections or "cross-sections") were cut using a sledge microtome (Model 860 Sledge Microtome, American Optical Corp., Buffalo, NY, USA). The cross-sections were stained with I_2KI (to show starch) and mounted in glycerol on microscope slides. Images of the cross-sections were taken at 100× or 200× magnification using a light microscope with an attached digital camera (Olympus BH-2, Olympus Imaging Corp., Center Valley, PA; Spot Insight 2, v. 18.2 Color Mosaic, Diagnostic Instruments, Inc., Sterling Heights, MI). Multiple (non-overlapping) images were taken of each cross section, with each image showing at least 200 cells. Our final dataset included 26 CCR, 22 CO, and 37 FCA images. The goal for this research project is to classify three functionally distinct plant cell types found in the xylem tissue (vessel, fiber, and parenchyma). Our objective is to construct a machine learning model that learns the features of these plant cell types alongside its surrounding characteristics to classify them with high accuracy. Flowering plants have two types of conductive tracheary elements: vessels

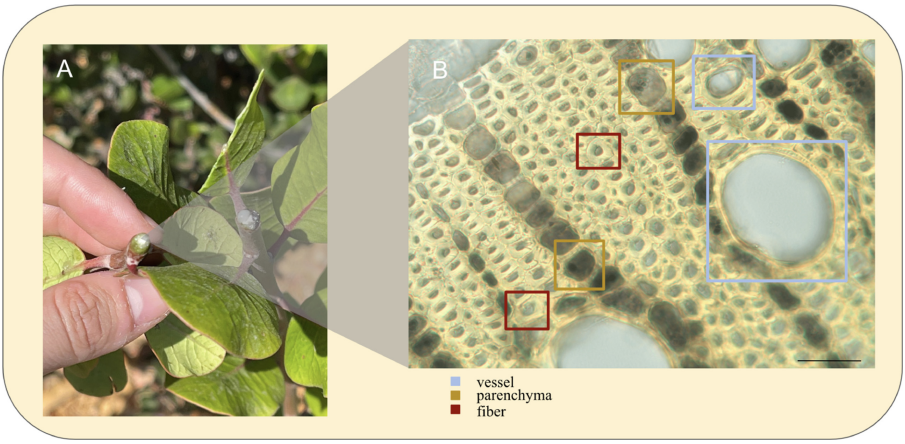

Fig. 1. (A) Chaparral shrub stem cut transversely as to prepare cross sections. (B) Micrograph of transverse cross section with labeled cell types. Boxes are placed as for cropping. Scale bar = 50 μm.

(typically larger diameter, composed of multiple cells) and tracheids (typically smaller diameter, composed of a single cell). However, it can be difficult to distinguish tracheids from other cell types in light micrographs, as large tracheids can appear similar to small vessels and small tracheids can appear similar to fibers. Thus, we did not attempt to identify tracheids in this study; we tried to avoid using images of tracheids. For labeled vessels, we selected large cells that were most likely vessels and not tracheids. However, it is possible that some tracheids were incorrectly labeled as vessels or fibers. Additionally, the roots of some shrubs contained gelatinous fibers, which are morphologically distinct from the more common sclerenchyma fibers. We categorized all fibers (gelatinous and sclerenchyma) as falling within the cell type class of "fibers" for this study. Finally, we did not distinguish between axial and ray parenchyma, but rather categorized them all within the cell type class of "parenchyma".

All of the original images were re-scaled to 1600×1200 for each image cross section regardless of the shrub species. We utilized a manual image cropping software called *makesense.ai* to crop the individual cells. We discarded all the extremely zoomed out images and chose the images with good resolution. Since vessels are the least abundant compared to fibers and parenchyma, we started with cropping the vessels and cropping approximately the same amount for fibers and parenchyma. The cells that are not fully shown in the image, i.e. are in the corner or blurry, were not cropped. This process is depicted in Fig. 1. This cropping process produced 790 unique images of vessels, fibers, and parenchyma cells.

When splitting our data into training and testing sets, our group decided to train a model on two shrub species and use the third species as an external validation. All models were run three times, with different species used as the test and training sets each time.

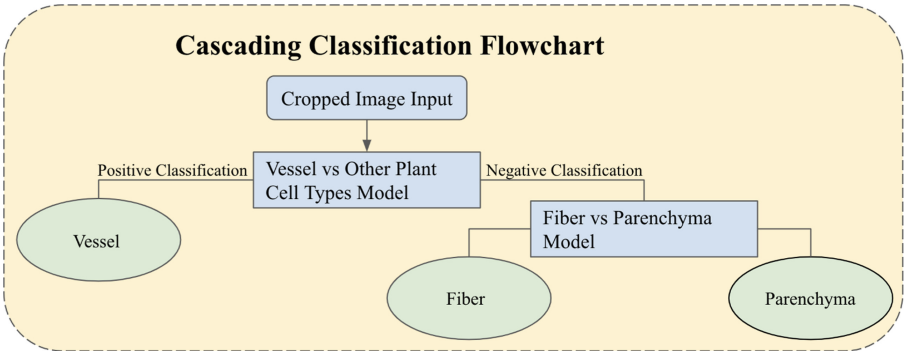

Fig. 2. Illustration of cascade-like framework to achieve a multi-class classification while avoiding its potential sub-class confusions. This is attained by splitting the classifier into two binary deep-learning classification models.

4 Methodology

Our research presents a cascade-like approach to classifying plant cell-types and consists of two separate models, each for their own classification task of varying complexity. Additionally to the cascade-like models, we then propose the effects of inputting two image inputs to the machine learning model- the first being a cropped image of either a vessel, fiber, or parenchyma, and the second being a broader image that displays some context around that cropped image.

4.1 Data Augmentation and Pre-processing

To mitigate the minute number of cropped training images that we obtained, some data augmentation was implemented to give our model more generalization. By using a PyTorch transform, each cropped cell type image was augmented in terms of a random rotation between 0 and 180° ten times.

Our data loading consists of a three step process of pre-processing the images. The first step is to resize each cropped image to $(224, 224)$ (width, height) pixels, as the pre-trained ResNet-18 was trained on this image size on ImageNet [25]. Following, we normalize the features in each of the data sets by calculating the mean and standard deviation for the data set as a whole and computing a z score standardization for each image, ultimately modifying each image to have roughly a mean of 0 and standard deviation of 1. Lastly, each pixel value in the RGB channels are transformed into a range spanning from 0–1 by a division of 255 through a PyTorch Tensor.

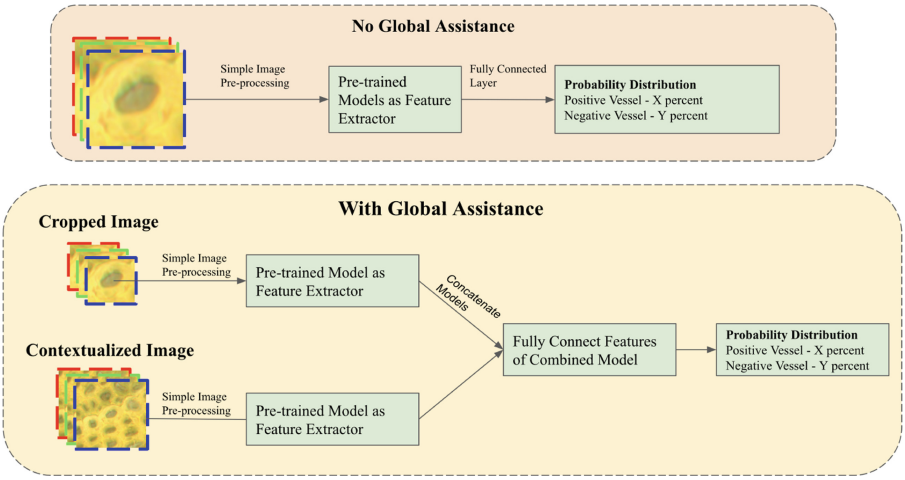

Fig. 3. Portrayal of our experiments of the advantages of an additional cropped image input to potentially enhance classification results.

4.2 Cascading-Like Model

Due to the fact that a multi-class cell type classification assignment may be harder for features to be classified, our group trained and optimized one model on categorizing vessels vs other cell types, and the other on classifying fibers vs parenchyma cells.

As depicted in Fig. 2, the intuition is to deliver a cropped cell image to two potential classification models. First, the cropped cell image will be sent to the a model that will classify it as a vessel or non-vessel. If the first model were to classify that cropped image was a vessel, then the classification task would be complete, however, in the case where the image is a non-vessel, then the second model will classify that cropped image as a fiber or parenchyma.

4.3 Global Contextualization Approach

While local patches can capture detailed information about the texture of a cell, it lacks the contextual information necessary to classify some cells. The reasoning behind this approach is due to the potential similarity of fiber and parenchyma cell class types when strictly cropped with little to no surrounding information, particularly for fibers and axial parenchyma. However, when including a secondary image with surrounding information, we hypothesize a preferable more concise model.

To achieve the contextualized photos, we took the image dimensions of each cropped plant cell image and re-cropped a new globalized image that is 140 pixels longer and taller than the original cropped image. As illustrated in Fig. 3, we decided to extract the features of the original cropped image and the globalized

cropped image separately in a chosen feature extraction model, then concatenate the features in a wrapper class where those added features are fully connected into a probability distribution of two classes.

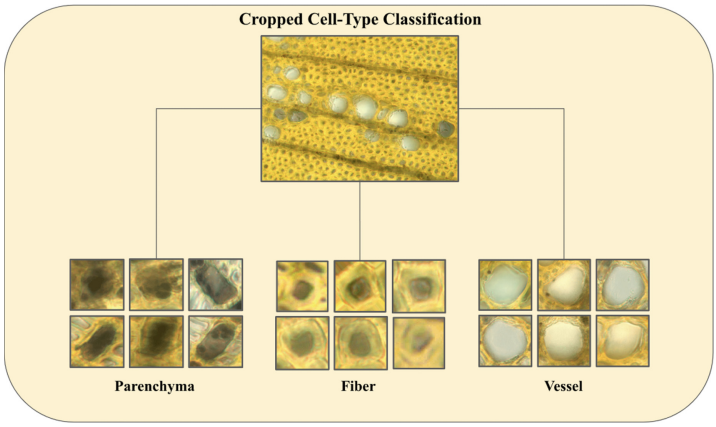

Fig. 4. Depiction of the cell-type classification we hope to achieve with deep learning.

5 Experiments and Results

To fulfill our research goal, we trained one pipeline that consists of two binary classification models that classifies one cropped plant cell type input, and a second pipeline consisting of two binary classification models, that classifies two image inputs as a plant cell type. For our baseline classification models, we appropriated three popular deep learning models: ResNet-18, VGG-16, and DeiT, as feature extractors by freezing the weights previously trained on ImageNet, and only training the fully connected layer [25–27].

For each model, our data was partitioned into three data sets. The training data, which was permuted to choose two of the three plant species for training and the third plant species as an external validation, was assigned an approximate $[90, 10]$ train-validation split after augmenting. This was done by implementing a random number generator, where on the $1/10th$ probability scenario, that image alongside its augmented counterparts would be sent to the validation data, which was subsequently used for hyper-parameter tuning. Figure 4 illustrates our end goal for classifying these xylem cell-types. We chose an initial learning rate of 0.1 and decreased it by a magnitude of 10 every n steps depending on the sub-problem we were trying to solve.

5.1 Model Evaluation Metric

The accuracy of each of our models are evaluated based on the number of predictions the model gets correct on the external test set divided by the length of

Table 1. These are the scores for each baseline pre-trained convolutional neural networks with the bare cropped image inputs, and the cropped image input with contextual assistance.

Baseline models	ResNet-18	VGG-16	DeiT
Vessel vs other cell types	96.7%	93.9%	97.1%
Vessel vs other cell types + large patches	98.1%	94.8%	98.1%
Fiber vs parenchyma	91.00%	76.4%	82.6%
Fiber vs parenchyma + large patches	91.7%	81.3%	86.8%

the test set. To find these predictions, we take the max of the probability distribution outputted by our machine learning model and count the overlapping corrects with our ground truth labels. To determine the overall accuracy of a cascade-like model, the average score of both sub-models are taken.

For our final models, we have decided to report results by a percentage of accuracy on the CCR plant species as the external test with an error margin calculated by the standard deviation of the CCR test accuracies, and the CO and FCA accuracies. By doing so, we hope to have created classification models that will yield similar test results within the error margin on other unseen species.

5.2 Baseline Results

To determine which pre-trained feature extractor to use, we trained both models without data augmentation on the three chosen neural networks (ResNet-18, VGG-16, DeiT) to determine initial results. Our group decided that ResNet-18 was the most accurate and efficient feature extractor for our research goals, because without any augmentation, it is clear that ResNet-18 has the best performance for all sub-problems. Additionally, the information shown in Table 1 starts to strengthens our claim of contextualized images providing classification assistance, as marginal improvements are evident in the contextualized image models.

5.3 Results

Our hypothesis of adding a contextualized image to the machine learning model proved to be accurate. Table 2 shows that adding a global patch for vessel classification improved the vessel vs non-vessels by 5.7% correctly classifying 211/213 vessels, fiber vs parenchyma by 2.8%, and escalating the overall accuracy by 4.2%. As a justification for our cascade-like architecture, the total accuracy of a trained and optimized multi-class classification model with data augmentation and global patch input is also visualized to be evidently worse than both the non-global patch and with global patch cascade-like models.

Table 2. A comparison of the performance of ResNet-18 with augmented images and global patches vs ResNet-18 with just data augmentation. Large patches are shown to increase classification accuracy. A justification for our cascading-like model is supported when compared with the multi-class classification results. Abbreviation Notes: (Ves, Fib, Par, aug) = (Vessel, Fiber, Parenchyma, augmentation

Cascading model	Ves. vs other	Fib. vs par.	Overall accuracy
Large patches + data aug.	99.1 ± 1.2%	97.2 ± 4.3%	98.1 ± 2.6%
Data aug.	93.4%	94.4%	93.9%
Non-cascading model	Ves. vs other	Fib. vs par.	Overall accuracy
Large patches + data aug.	x	x	90.1%

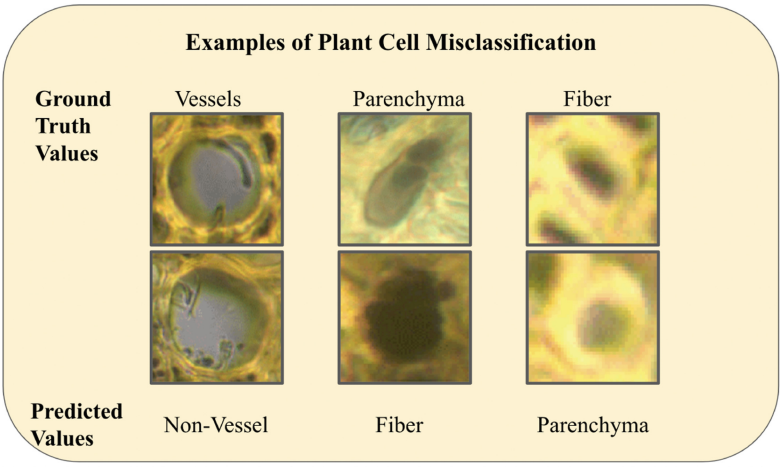

Fig. 5. Representation of the cropped plant cell images that were misclassified by our model

6 Discussion

In this study, we used a novel application of machine learning to classify plant cell types in xylem tissue. We discovered that applying two cascading models (vessels vs non-vessels and fibers vs parenchyma) achieved more accurate results than a single model to classify the three cell types. Vessels have a more distinctive shape compared to fibers and parenchyma, which likely explains why the accuracy score in the first model is higher than in the second model comparing fibers and parenchyma. We ran the cascading models three times and found some variation depending on which two species were used for training and which one species was used for testing the model. This likely reflects interspecific variation in cell characteristics and the cell types present (e.g., the lack of tracheids in FCA) and the challenge of fine-tuning a model that can be accurately applied to a broad selection of species.

Additionally, we discovered that incorporating the larger context ("patches") surrounding each plant cell improved the accuracy of our classification model. The appearance and size of plant cells is naturally variable within cell types (even within a single image), due to a variety of genetic, environmental, or developmental factors. Thus, the context can greatly increase the confidence in cell classification (e.g., vessels are larger than fibers). Also, some cell types can be classified based on the pattern that they form within the tissue. For example, parenchyma in xylem tissue form lines ("rays") through the fibers and vessels, as shown in Fig. 1. Future models may be able to incorporate contextual information with even greater success.

Another challenge to our current framework is that some cells would overlap with other cells in the cropped rectangular frame which may cause the machine to analyze the undesired overlapping cell as part of the region of interest for classification. When cropping parenchyma for instance, the parenchyma that is directly next to it would sometimes appear in the cropped frame. As illustrated in Fig. 5, our model misclassified some parenchyma, fibers, and vessels, whether it be due to a lack of image quality, or similarity in features. In our future work, we may try to implement a cropping technique that is similar to the magnetic lasso tool that would crop the cell at its exact borders.

While promising, our current framework could be expanded and diversified. For example, we could train and test this model using images from more species, more developmental stages, and grown under a greater variety of environmental conditions. While some cell characteristics are fairly conserved within a cell type, there is an incredible amount of morphological diversity within and among species. Future studies may determine whether our model can be broadly applied across ecosystems, growth forms (e.g., woody vs non-woody tissue), and organs (e.g., stem vs root).

Our cascading model framework could also be applied to classify a greater number of cell types. For this study, we adopted a simplified classification system for the three most abundant cell type classes (vessel, fiber, and parenchyma). However, future models may further distinguish cell types, such as between ray vs axial parenchyma, libriform vs gelatinous fibers, and vessels vs tracheids. A more detailed model would also likely benefit from the cascading model framework and contextual information.

7 Conclusion

Our study produced a novel approach to classifying plant cell types from light micrographs with high accuracy. Our model may provide a foundation for future models that are capable of detecting, classifying, and measuring plant cells from unprocessed light micrographs. Our framework might also be applied to other times of image datasets, such as micro-computed tomography. With the increasing availability of large image datasets, such a model would greatly broaden the utility of these resources for research teams that lack the manpower for manual analysis.

Acknowledgements. We would like to thank the Keck Foundation for their grant to Pepperdine University to support our Data Science program. We would also like to thank R. Brandon Pratt for help with shrub sample collection.

References

1. Rundel, P.W.: California chaparral and its global significance. In: Underwood, E.C., Safford, H.D., Molinari, N.A., Keeley, J.E. (eds.) Valuing Chaparral. SSEM, pp. 1–27. Springer, Cham (2018). https://doi.org/10.1007/978-3-319-68303-4_1
2. Jacobsen, A.L., Pratt, R.B., Ewers, F.W., Davis, S.D.: Cavitation resistance among 26 chaparral species of southern California. Ecol. Monogr. **77**(1), 99–115 (2007)
3. Davis, S.D., Ewers, F.W., Sperry, J.S., Portwood, K.A., Crocker, M.C., Adams, G.C.: Shoot dieback during prolonged drought in Ceanothus (Rhamnaceae) chaparral of California: a possible case of hydraulic failure. Am. J. Bot. **89**(5), 820–828 (2002)
4. Venturas, M.D., MacKinnon, E.D., Dario, H.L., Jacobsen, A.L., Pratt, R.B., Davis, S.D.: Chaparral shrub hydraulic traits, size, and life history types relate to species mortality during California's historic drought of 2014. PLoS ONE **11**(7), e0159145 (2016)
5. Pratt, R.B., Jacobsen, A.L.: Conflicting demands on angiosperm xylem: tradeoffs among storage, transport and biomechanics. Plant, Cell Environ. **40**(6), 897–913 (2017)
6. Pratt, R., Jacobsen, A., Ewers, F., Davis, S.: Relationships among xylem transport, biomechanics and storage in stems and roots of nine Rhamnaceae species of the California chaparral. New Phytol. **174**(4), 787–798 (2007)
7. Jacobsen, A.L., Agenbag, L., Esler, K.J., Pratt, R.B., Ewers, F.W., Davis, S.D.: Xylem density, biomechanics and anatomical traits correlate with water stress in 17 evergreen shrub species of the Mediterranean-type climate region of South Africa. J. Ecol. **95**(1), 171–183 (2007)
8. Davis, S.D., Sperry, J.S., Hacke, U.G.: The relationship between xylem conduit diameter and cavitation caused by freezing. Am. J. Bot. **86**(10), 1367–1372 (1999)
9. Hacke, U.G., Sperry, J.S.: Functional and ecological xylem anatomy. Perspect. Plant Ecol. Evol. Syst. **4**(2), 97–115 (2001)
10. Pittermann, J., Sperry, J.S.: Analysis of freeze-thaw embolism in conifers. The interaction between cavitation pressure and tracheid size. Plant Physiol. **140**(1), 374–382 (2006)
11. Hacke, U.G., Sperry, J.S., Pockman, W.T., Davis, S.D., McCulloh, K.A.: Trends in wood density and structure are linked to prevention of xylem implosion by negative pressure. Oecologia **126**(4), 457–461 (2001). https://doi.org/10.1007/s004420100628
12. Jacobsen, A.L., Ewers, F.W., Pratt, R.B., Paddock, W.A., III., Davis, S.D.: Do xylem fibers affect vessel cavitation resistance? Plant Physiol. **139**(1), 546–556 (2005)
13. Pratt, R.B., et al.: Starch storage capacity of sapwood is related to dehydration avoidance during drought. Am. J. Bot. **108**(1), 91–101 (2021)
14. Biswas, S., Barma, S.: A large-scale optical microscopy image dataset of potato tuber for deep learning based plant cell assessment. Sci. Data **7**(1), 1–11 (2020)
15. Nissim, N., Dudaie, M., Barnea, I., Shaked, N.T.: Real-time stain-free classification of cancer cells and blood cells using interferometric phase microscopy and machine learning. Cytometry A **99**(5), 511–523 (2021)

16. Ding, S., et al.: Predicting heart cell types by using transcriptome profiles and a machine learning method. Life **12**(2), 228 (2022)
17. Abdullah, E., Turan, M.K.: Classifying white blood cells using machine learning algorithms. Int. J. Eng. Res. Dev. **11**(1), 141–152 (2019)
18. Ziemińska, K., Westoby, M., Wright, I.J.: Broad anatomical variation within a narrow wood density range–a study of twig wood across 69 Australian angiosperms. PLoS ONE **10**(4), e0124892 (2015)
19. Ramesh, S., Hebbar, R., Niveditha, M., Pooja, R., Shashank, N., Vinod, P., et al.: Plant disease detection using machine learning. In: 2018 International Conference on Design Innovations for 3Cs Compute Communicate Control (ICDI3C), pp. 41–45. IEEE (2018)
20. Priya, C.A., Balasaravanan, T., Thanamani, A.S.: An efficient leaf recognition algorithm for plant classification using support vector machine. In: International Conference on Pattern Recognition, Informatics and Medical Engineering (PRIME-2012), pp. 428–432. IEEE (2012)
21. Wolny, A., et al.: Accurate and versatile 3D segmentation of plant tissues at cellular resolution. Elife **9**, e57613 (2020)
22. Vu, Q.D., et al.: Methods for segmentation and classification of digital microscopy tissue images. Front. Bioeng. Biotechnol. **7**, 53 (2019)
23. Garcia-Pedrero, A., et al.: Convolutional neural networks for segmenting xylem vessels in stained cross-sectional images. Neural Comput. Appl. **32**(24), 17927–17939 (2020). https://doi.org/10.1007/s00521-019-04546-6
24. Resente, G., et al.: Mask, train, repeat! Artificial intelligence for quantitative wood anatomy. Front. Plant Sci. **12**, 767400 (2021)
25. He, K., Zhang, X., Ren, S., Sun, J.: Deep residual learning for image recognition. In: Proceedings of the IEEE Conference on Computer Vision and Pattern Recognition, pp. 770–778 (2016)
26. Tammina, S.: Transfer learning using VGG-16 with deep convolutional neural network for classifying images. Int. J. Sci. Res. Publ. (IJSRP) **9**(10), 143–150 (2019)
27. Touvron, H., Cord, M., Douze, M., Massa, F., Sablayrolles, A., Jégou, H.: Training data-efficient image transformers & distillation through attention. In: International Conference on Machine Learning, PMLR, pp. 10347–10357 (2021)